

## PRELIMINARY TESTS OF MECHANICAL ABUSE - NAIL TESTS OF LIBS

<sup>1,3</sup>Papurello Davide, <sup>1</sup>Braghiroli Beatrice, <sup>2,3</sup>Bodoardo Silvia, <sup>2,3</sup>Amici Julia, <sup>1,3</sup>Borchiellini Romano

<sup>1</sup>Department of Energy (DENERG), Politecnico di Torino, IT

<sup>2</sup>Department of Applied Science and Technology (DISAT), Politecnico di Torino, IT

<sup>3</sup>Energy Center, Politecnico di Torino, IT

DOI 10.3217/978-3-85125-996-4-22 (CC BY-NC 4.0)

This CC license does not apply to third party material and content noted otherwise.

### ABSTRACT

Current tunnel safety concepts are based on the experience of conventional fuel vehicle accidents. The transition in the coming years will involve the use of alternative fuels such as hydrogen, natural gas and the use of electric vehicles. Among them, it seems that in the near future medium-sized and small vehicles will be powered electrically by lithium-ion batteries (city cars). The main problem of electric vehicles with Lithium-Ion batteries (LIBs) lies in the heat release rate (HRR), and toxic compounds released by LIB fire. Thermal runaway to a fire can be triggered by temperature, electricity, and mechanical abuse. The latter is more complex to manage via the Battery Management System (BMS) or cell architecture. In the present work, preliminary results of LIBs tested by nail test, inside a calorimeter are shown. The LIB cell tested and modelled is a SAMSUNG INR-18650-29E. Such a cell was tested at 100% SOC reaching temperatures above 800 °C and a maximum pressure value of about 4 bar. The concentration of CO inside the chamber was measured. The measured CO level ranged from 3000-4000 ppm(v), comparable to other research. The model implemented on COMSOL consists of two components: a 1D model that aims to simulate the electrochemical behaviour of the battery through a pseudo-two-dimensional (p2D) model, while the 3D model simulates heat transfer only.

*Keywords: LIB; BEV; HRR; Toxic release*

### 1. INTRODUCTION

Lithium Ion Batteries (LIBs) have become one of the most popular energy storage technologies in recent years, powering a wide range of devices and applications, from Portable Electronic Devices (PEDs) to Electric Vehicles (EVs) [1]. Electric vehicles are defined according to IEC 61851-1 [2]. EVs are defined, according to the Standard IEC 61851-1 and the main rechargeable storage systems considered are LIBs. The market increase is linked to the ongoing clean energy transition. In fact, with the possibility of using renewable energy to charge EVs, even locally, and zero emissions during operation, EVs are seen as a viable way to substitute conventional Internal Combustion Engine (ICE) vehicles. Moreover, EVs are characterized by up to four times higher energy efficiency than ICE vehicles [3], which is also possible to further increase by using regenerative braking. As the use of batteries has increased [4], a greater demand has been placed on their safety and management. Whether the application, safety of batteries is of paramount importance to manufacturers and integrators, especially in the event of external mechanical stress or Thermal Runaway (TR). Abuse testing is a crucial aspect of LIBs safety and reliability, as it helps to understand battery failure mechanisms, identify potential hazards and improve safety measures [5–7]. Abuse tests are divided into mechanical, electrical and thermal [8]. Among different abuse tests, nail penetration is a common mechanical test that consists of the penetration of the battery using a

sharp object [9]. This type of test is helpful to study the mechanical crash via an internal short circuit. To reduce the number of experimental tests, as they are destructive and can be expensive, it is important to model the abuse process. Furthermore, this can help to develop a predictive capability of the TR battery's response to mechanical impacts and, consequently, develop prevention and mitigation approaches to ensure the safety of the battery system. These results will be used in future activities aimed at larger vehicles (scale effect).

## 2. MATERIAL AND METHODS

The nail penetration test is an industry-standard method for simulating an Internal Short Circuit in a cell (ISC). It is performed by using an electrically conductive pointed rod to pierce the battery perpendicularly to the battery. Typical nail diameters range from 3 mm to 8 mm, depending on the standard considered, and the penetration speed is typically 8 cm/s [9–13]. The test is considered successful if the cell does not explode or burn. Several variables can be considered such as: State Of Charge (SOC), chemistry, geometry, nail speed, penetration depth, position, nail material, nail diameter, and cell orientation. Some of the previous variables can affect the fire release, as demonstrated by [14]. The nail penetration tests have been performed using the Thermal Hazard Technology EV+ Accelerating Rate Calorimeter (ARC, THT, UK) provided with the auxiliary option called Nail Penetration and Crush Option (NPCO) present at the Energy Center facility.

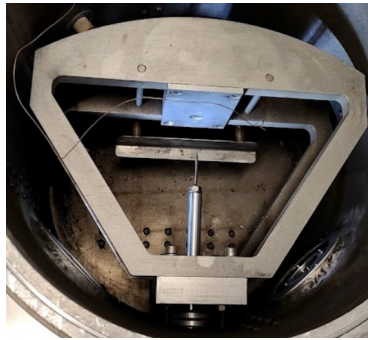


Figure 1: NPCO at the Energy Center.

Table 1 shows the main properties of the INR18650-29E battery model tested. It is produced by Samsung SDI Co., Ltd.

Table 1: Details for the LIB 18650 tested

Specification	INR18650-29E[15]
Type (-)	Cylindrical
Diameter (mm)	18
Height (mm)	65
Nominal capacity (mAh)	2850
Nominal voltage (V)	3.65
Charging voltage (V)	4.2 +/- 0.05
Charging method (-)	CC-CV
Charging current (mA)	1375 (Standard)
Charging time (hours)	3
Discharge Cut-off Voltage (V)	2.5
Cell weight (g)	48
Operating temperature (°C)	25 °C

The cathode is made of Nickel Manganese Cobalt (NMC) coated onto an aluminium current collector, while the anode is made of graphite. The electrolyte is liquid and based on LiPF<sub>6</sub> and organic solvents. The CC-CV method was used to reach the SOC 100%. The battery is positioned in the holder to ensure the penetration in the centre of the battery. All tests have been performed using an AISI 316 stainless steel nail, with a diameter equal to 4 mm that penetrates the battery at a nail speed equal to 80 mm/s starting 35 mm from the battery. The battery is kept in the ARC until a small enough temperature is reached (Cool temperature equal to 35 °C), after which it is possible to open the calorimeter with precaution. The test is repeated twice for each battery. IR camera (THT, UK) is used to monitor the temperature distribution, while a k-type thermocouple (Tersid srl, Italy) is placed near the centre of the battery. A pressure transducer is mounted in the calorimeter with a pressure range of 0 – 200 bar and a resolution of 0.005 bar, precision of 0.02% and accuracy of 0.05% [16]. Gas exhausts are measured in the canister using the Testo 330 (Testo SE & Co. KGaA, Germany) to monitor the CO production (CO 0 – 10000 ppm(v), +/- for 5% 200 – 2000 ppm(v) and +/- 10% for 2000 – 10000 ppm(v) with 4 s of reaction time).

The model has been implemented into COMSOL Multiphysics® software v6.0 using the Battery Design Module functionalities coupled to the Heat Transfer in Solids interface. The model consists of a coupled p2D electrochemical-3D thermal.

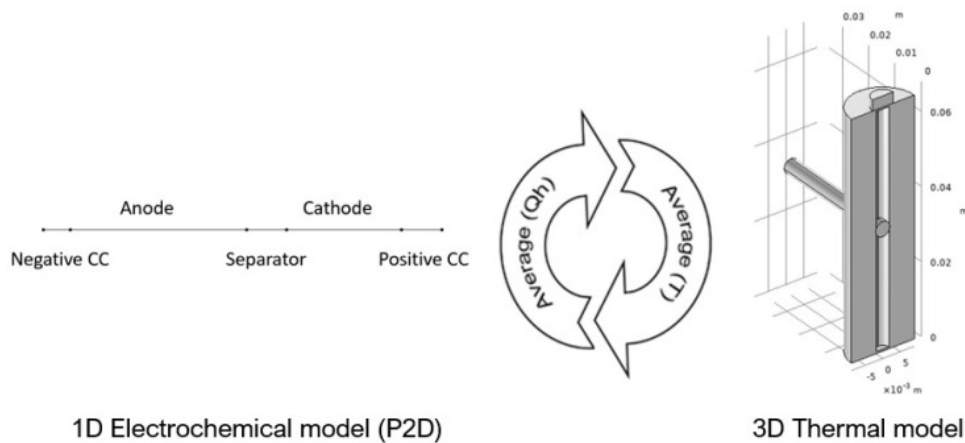


Figure 2: Model structure and schematic representation.

A 1D component is used to solve the P2D model, while a 3D component solves the thermal equations. This separation between electrochemical and thermal equations is carried out to obtain faster computational times with lower CPU requirements concerning a fully 3D electrochemical-thermal model.

### 3. RESULTS AND DISCUSSION

#### 3.1. Experimental test abuses

During the tests, the temperature and pressure of the sample and their rate of change are recorded over time. The data obtained for all tests are analysed and compared. The test starting temperature is set at 20 °C. The maximum temperatures reached are 469 °C and 584.3 °C for Test3\_29 and Test4\_29, respectively. The graphs show a sharp increase after about one second, followed by a rapid decrease until a plateau is reached. Test 3\_29E and Test 4\_29E (in blue and orange in the graph, respectively) have a very similar shape: the temperature rises sharply, then appears to slow down but then rises rapidly again reaching its peak in about 1 minute.

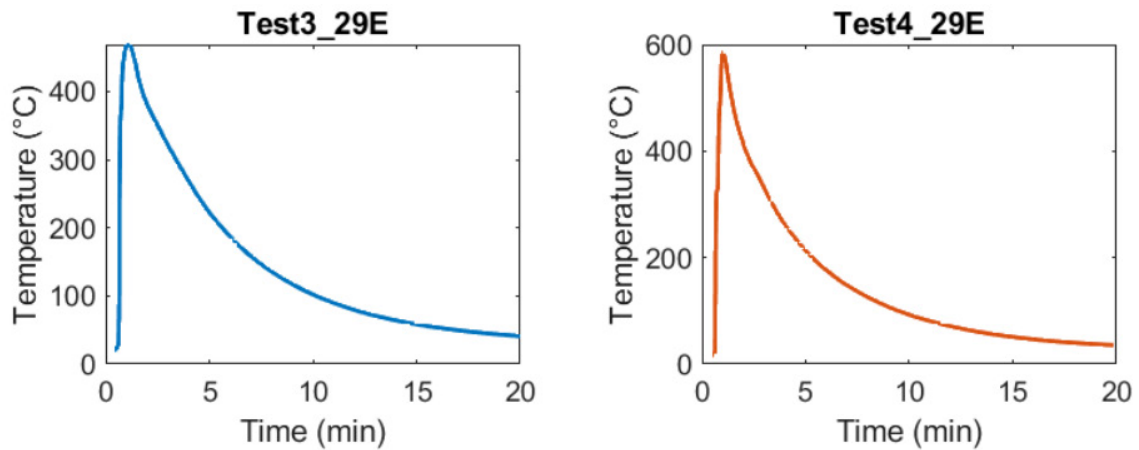


Figure 3: Battery 29E results in terms of temperature.

The IR camera was used to see the TR evolution in time (5 s per frame), see the following figure. It is possible to see the nail penetrated and the instantaneous increase of the temperature. Being an IR camera, it is only possible to appreciate the qualitative increase in thermal energy of a rapid process. This aspect is important to emphasize the need to improve data acquisition time.

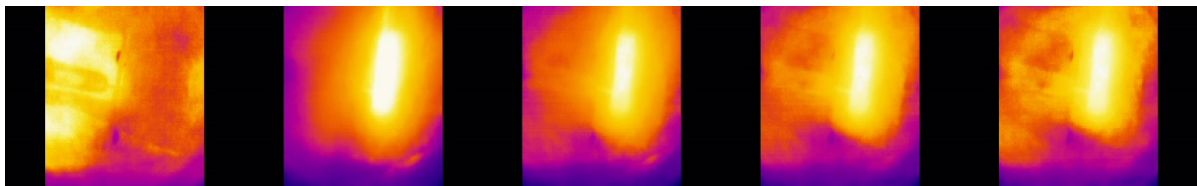


Figure 4: battery 29E IR camera, TR evolution, each frame was recorded every 5s.

The abuse test led to the TR being observed, causing the battery to explode, see the figure below.



Figure 5: battery 29E after the nail penetration test.

The tests reported above show rapid changes in pressure, followed by an almost stable state condition. The highest-pressure value recorded was 3.57 bar.

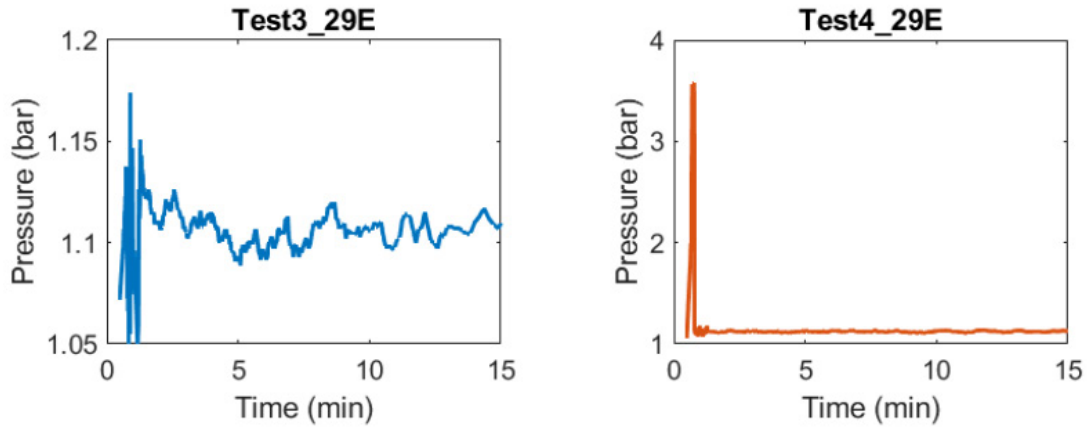


Figure 6: Battery 29E results in terms of pressure.

The following figure shows the trend of CO emitted during the TR. A maximum CO value of about 4000 ppm(v) was reached, and similar results have been published in the literature [17]. The development of CO is related to the establishment of incomplete combustion as a result of thermal runaway of the battery.

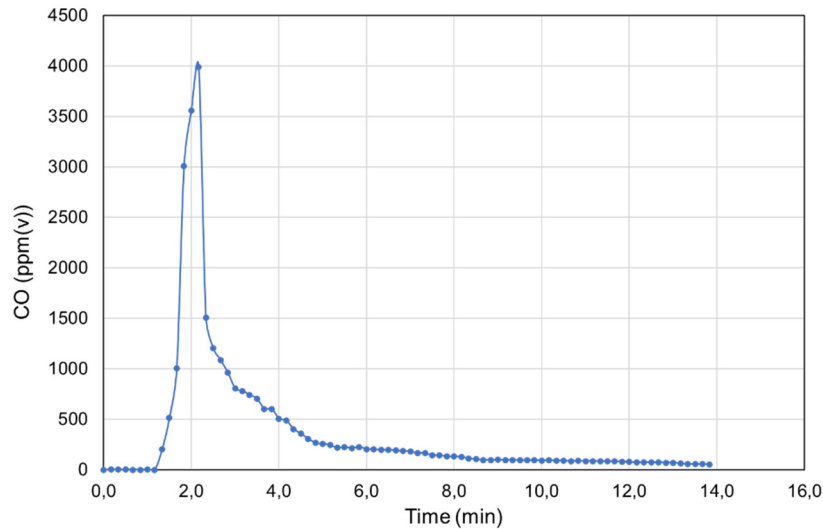


Figure 7: Battery 29E results in terms of CO release (Test3\_29E).

### 3.2. Model results

The model implemented on COMSOL consists of two components: a 1D model that aims to simulate the electrochemical behaviour of the battery through a p2D model, while the 3D model simulates heat transfer only. To implement the TR phenomenon the parameters used are reported in the following table.

Table 2: Exothermic reaction parameters

Reaction	H (J/Kg)	W (Kg/m <sup>3</sup> )	A (s <sup>-1</sup> )	E (J mol <sup>-1</sup> )
SEI decomposition	$2.57 \times 10^5$	610	$1.14 \times 10^{14}$	$1.35 \times 10^5$
Anode-Electrolyte	$1.714 \times 10^6$	610	$7.18 \times 10^{13}$	$1.35 \times 10^5$
Cathode-Electrolyte	$3.14 \times 10^5$	1120	$6.66 \times 10^{13}$	$1.41 \times 10^5$
Electrolyte decomposition	$1.55 \times 10^5$	406.9	$5.12 \times 10^{15}$	$1.75 \times 10^5$

The nonlocal coupling operator was used to couple the 1D electrochemical model and the 3D model. As shown in the figure below, the temperature starts to rise around the nail, generating a hot spot. After about 30 s, the temperature reached is homogeneous.

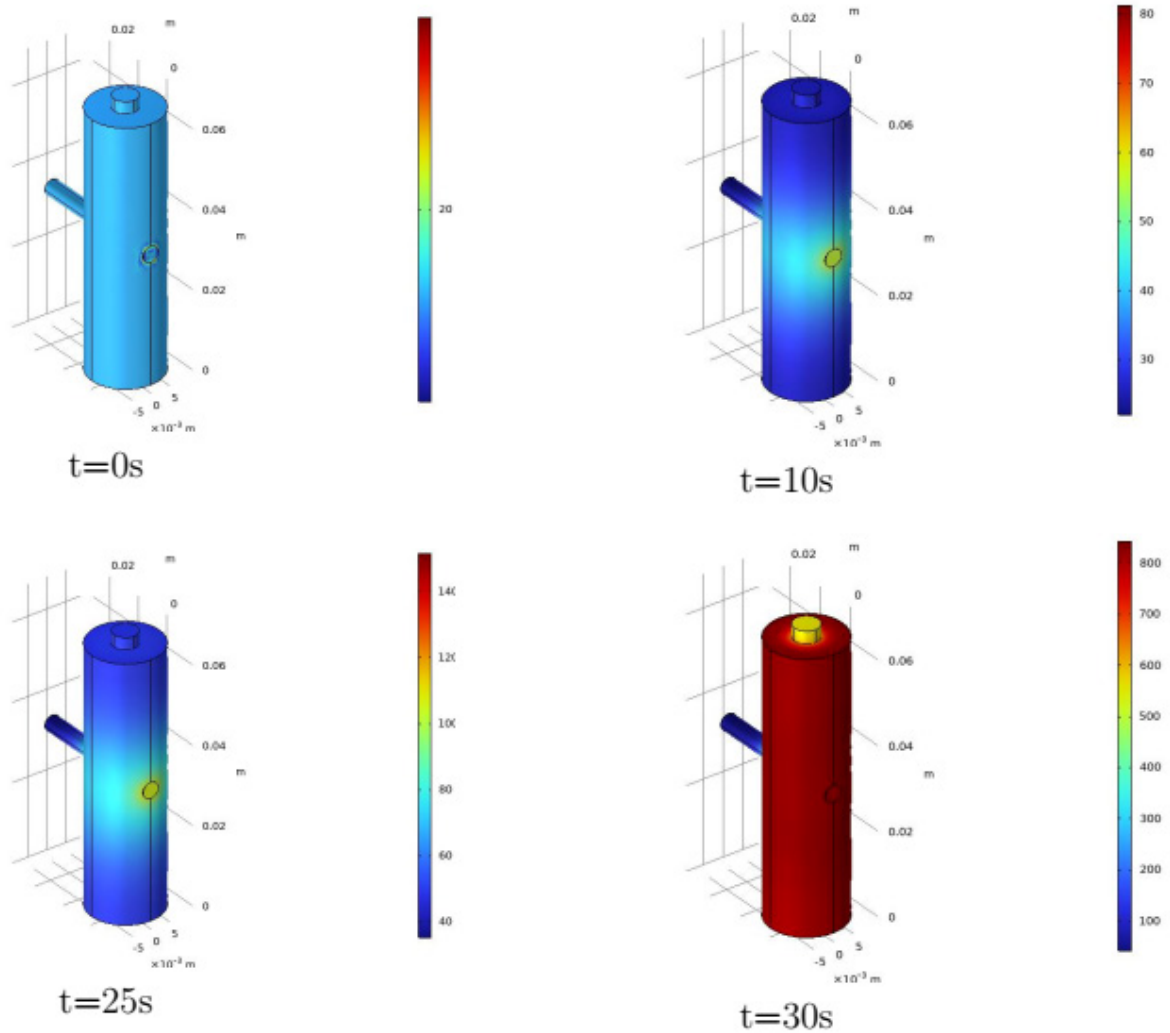


Figure 8: Nail penetration test modelled with Comsol (Test3\_29E).

The maximum temperature monitored during the reported experimental tests is approximately over 600 °C, while the maximum temperature reached by the model is just over 700 °C. The experimental variability of the maximum temperature value is very high. An increase in the number of samples tested could improve the validity of the data by improving the validation of the model.

At this point considering the structure of the battery and the data sheet provided by the manufacturer [15], it is possible to assess the power generated during mechanical abuse, by following these equations:

$$Q_{heat} = \rho \cdot C_p \cdot \frac{\partial T}{\partial t} \text{ (eq.1)}$$

$$\rho_{batt} = \frac{\sum L_i \rho_i}{\sum L_i} \text{ (eq.2)}$$

$$C_{p, batt} = \frac{\sum L_i C_{p, i}}{\sum L_i} \text{ (eq.3)}$$

Where:  $\rho$  is the weighted density ( $\text{kg/m}^3$ ) for the LIB material,  $C_p$  is the heat capacity ( $\text{kJ/K}$ ),  $\partial T/\partial t$  is the thermal gradient recorded during the experimental test and  $L_i$  is the  $i$ -layer considered.

The results show that the single battery with a nominal capacity of 2.85 Ah can produce up to a maximum heat output of 300 W during the nail test. This value is not an outlier because of the rapid reaction of the TR, but it will be necessary to refine the collection of times to seconds as an order of magnitude to collect more data.

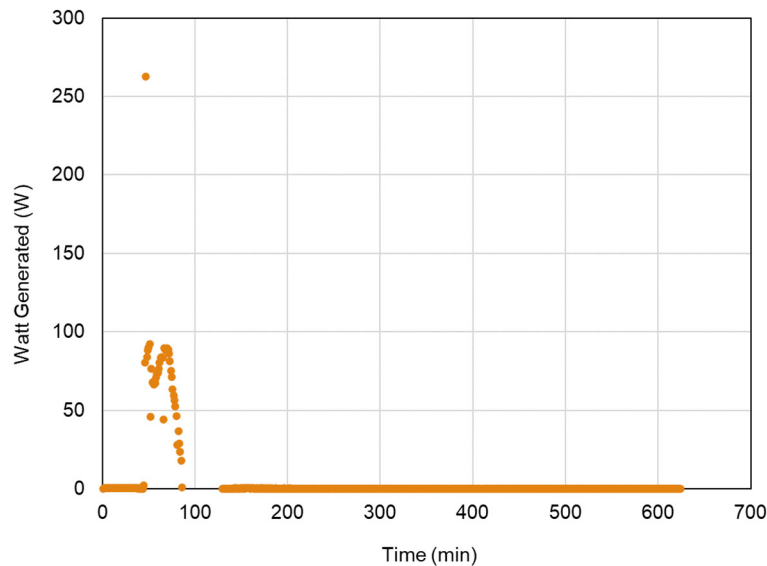


Figure 9: Thermal power generated during the nail test.

#### 4. CONCLUSION

The nail test was investigated as the mechanical abuse condition for a commercial Lithium ion cell. The experimental results were used to monitor the temperature, pressure and the gas exhausts released. The maximum temperature recorded experimentally vary from 400 to above 600 °C, while the model implemented show a maximum temperature roughly around 700 °C. The experimentally recorded maximum temperature ranges from 400 to over 600 °C, while the implemented model shows a maximum temperature approximately around 700 °C. The experimental activity should be improved by increasing the number of trials to reduce the temperature variability. Regarding the SOC effect, the higher the SOC, the greater the battery response, in terms of peak temperature. In terms of nail speed, a higher nail speed generally means a higher temperature. Also, in terms of voltage, the decrease to zero occurs faster with a higher nail speed. Experimental results obtained at a preliminary level will be used to validate models closer to real conditions. Gas analysis to detect the main toxic compounds (HF, HCl, HCN etc.) will have to be implemented. These results will be used to assess performance under battery pack abuse conditions, thus scaling up to higher electrical capacity sizes.

## 5. REFERENCES

- [1] S. S. Rangarajan, S.P. Sunddararaj, A.V.V. Sudhakar, C.K. Shiva, U. Subramaniam, E.R. Collins, T. Senjyu, Lithium-Ion Batteries—The Crux of Electric Vehicles with Opportunities and Challenges, *Clean Technologies*. 4 (2022) 908–930. <https://doi.org/10.3390/cleantechnol4040056>.
- [2] E. Standards, BS EN IEC 61851-1:2019 Electric vehicle conductive charging system General requirements, <https://www.en-standard.eu>. (n.d.). <https://www.en-standard.eu/bs-en-iec-61851-1-2019-electric-vehicle-conductive-charging-system-general-requirements/> (accessed November 16, 2023).
- [3] R.T. Yadlapalli, A. Kotapati, R. Kandipati, C.S. Koritala, A review on energy efficient technologies for electric vehicle applications, *Journal of Energy Storage*. 50 (2022) 104212. <https://doi.org/10.1016/j.est.2022.104212>.
- [4] Trends in batteries – Global EV Outlook 2023 – Analysis, IEA. (n.d.). <https://www.iea.org/reports/global-ev-outlook-2023/trends-in-batteries> (accessed November 16, 2023).
- [5] P.A. Christensen, Z. Milojevic, M.S. Wise, M. Ahmeid, P.S. Attidekou, W. Mroziak, N.A. Dickmann, F. Restuccia, S.M. Lambert, P.K. Das, Thermal and mechanical abuse of electric vehicle pouch cell modules, *Applied Thermal Engineering*. 189 (2021) 116623. <https://doi.org/10.1016/j.applthermaleng.2021.116623>.
- [6] C.F. Larsson, Lithium-ion Battery Safety - Assessment by Abuse Testing, Fluoride Gas Emissions and Fire Propagation, Chalmers University of Technology, 2017. <https://research.chalmers.se/en/publication/251352> (accessed October 3, 2022).
- [7] F. Larsson, P. Andersson, B.-E. Mellander, Lithium-Ion Battery Aspects on Fires in Electrified Vehicles on the Basis of Experimental Abuse Tests, *Batteries*. 2 (2016) 9. <https://doi.org/10.3390/batteries2020009>.
- [8] X. Feng, M. Ouyang, X. Liu, L. Lu, Y. Xia, X. He, Thermal runaway mechanism of lithium ion battery for electric vehicles: A review, *Energy Storage Materials*. 10 (2018) 246–267. <https://doi.org/10.1016/j.ensm.2017.05.013>.
- [9] B. Mao, H. Chen, Z. Cui, T. Wu, Q. Wang, Failure mechanism of the lithium ion battery during nail penetration, *International Journal of Heat and Mass Transfer*. 122 (2018) 1103–1115. <https://doi.org/10.1016/j.ijheatmasstransfer.2018.02.036>.
- [10] A.V. Shelke, J.E.H. Buston, J. Gill, D. Howard, K.C. Abbott, S.L. Goddard, E. Read, G.E. Howard, A. Abaza, B. Cooper, J.X. Wen, Characterizing and predicting 21700 NMC lithium-ion battery thermal runaway induced by nail penetration, *Applied Thermal Engineering*. 209 (2022) 118278. <https://doi.org/10.1016/j.applthermaleng.2022.118278>.
- [11] X. Gao, Y. Jia, W. Lu, Q. Wu, X. Huang, J. Xu, Mechanistic understanding of reproducibility in nail penetration tests, *Cell Reports Physical Science*. 4 (2023) 101542. <https://doi.org/10.1016/j.xcrp.2023.101542>.
- [12] N. Mao, S. Gadkari, Z. Wang, T. Zhang, J. Bai, Q. Cai, A comparative analysis of lithium-ion batteries with different cathodes under overheating and nail penetration conditions, *Energy*. 278 (2023) 128027. <https://doi.org/10.1016/j.energy.2023.128027>.
- [13] J. Diekmann, S. Doose, S. Weber, S. Münch, W. Haselrieder, A. Kwade, Development of a New Procedure for Nail Penetration of Lithium-Ion Cells to Obtain Meaningful and Reproducible Results, *J. Electrochem. Soc.* 167 (2020) 090504. <https://doi.org/10.1149/1945-7111/ab78ff>.
- [14] Z. Huang, H. Li, W. Mei, C. Zhao, J. Sun, Q. Wang, Thermal Runaway Behavior of Lithium Iron Phosphate Battery During Penetration, *Fire Technol.* 56 (2020) 2405–2426. <https://doi.org/10.1007/s10694-020-00967-1>.
- [15] INR18650-29E datasheet, (n.d.). <https://datasheetspdf.com/pdf-file/821874/Samsung/INR18650-29E/1> (accessed November 21, 2023).
- [16] EV+ Accelerating Rate Calorimeter | Thermal Hazard Technology, (n.d.). <https://www.thermalhazardtechnology.com/battery-products/ev-plus-accelerating-rate-calorimeter> (accessed November 22, 2023).
- [17] P. Ribière, S. Grugeon, M. Morcrette, S. Boyanov, S. Laruelle, G. Marlair, Investigation on the fire-induced hazards of Li-ion battery cells by fire calorimetry, *Energy Environ. Sci.* 5 (2012) 5271–5280. <https://doi.org/10.1039/C1EE02218K>.